Topological solitons in helical strings

Cristiano Nisoli[1,*] and Alexander V. Balatsky[1,2]

[1]*Theoretical Division and Institute for Material Sciences, Los Alamos National Laboratory, Los Alamos, New Mexico 87545, USA*

[2]*Nordita, KTH Royal Institute of Technology and Stockholm University, Stockholm, Sweden*

(Received 25 November 2014; revised manuscript received 14 March 2015; published 25 June 2015)

The low-energy physics of (quasi)degenerate one-dimensional systems is typically understood as the particle-like dynamics of kinks between stable, ordered structures. Such dynamics, we show, becomes highly nontrivial when the ground states are topologically constrained: a dynamics *of the domains* rather than *on the domains* which the kinks separate. Motivated by recently reported observations of charged polymers physio-adsorbed on nanotubes, we study kinks between helical structures of a string wrapping around a cylinder. While their motion cannot be disentangled from domain dynamics, and energy and momentum is not concentrated in the solitons, the dynamics of the domains can be folded back into a particle-like description of the local excitations.

DOI: 10.1103/PhysRevE.91.062601 PACS number(s): 61.41.+e, 87.15.−v, 03.65.Vf, 11.15.−q

I. INTRODUCTION

The relationship between topological and physical properties [1–3] has received much recent attention. It is relevant to elasticity [3,4], nonlinear physics [5,6], soft and hard condensed matter [2,3,7], and quantum computing [8,9]. As topology is the study of invariance under homeomorphism, it shines a light on continuum field theories. Topological invariants associated with physical objects often dictate interaction: for instance punctures in a plane (defects, dislocations, vortices) define a topological invariant (the winding angle) and thus a logarithmic field which, not surprisingly, also mediates their mutual interaction [4]. Similarly, topologically distinct states support infinitely continuum transitions [10,11].

We have previously investigated [11] the statistical mechanics (and connections with conformal invariance in quantum mechanics) of topological transitions among winding states representing winding and unwinding polymers. Here we study the Newton dynamics of a string (polymer) which has preferred winding directions around a cylinder (nanotube), coming for instance from screened self-interaction. If strings are stable in different, and not necessarily degenerate, helical structures, they exhibit topological solitons whose dynamics, however, is not "contained" in the kink but rather involves the entire system. This is a feature of the topology of helical solitons found also in systems of essentially different physics: in "dynamical phyllotaxis" [12–14] repulsive particles in cylindrical geometries mimic botanical patterns of leaves on stems, spines on cactuses, and petals on a flower [15] by self-organizing in helical lattices described by Fibonacci numbers [12,16], also separated by kinks; or in colloidal crystals on cylinders and rod-shaped bacterial cell walls [17].

While our analysis elucidates an interesting case of topology-dictated dynamics connected to the simplest topological invariant—the winding number—it is not without practical implications. Polymer-nanotube hybrids, ssDNA-carbon nanotubes in particular [18–21], have been the subject of much recent experimental and numerical research [18–28] as promising candidates for nanotechnological applications in biomolecular and chemical sensing, drug delivery [18,29], and dispersion and patterning of carbon nanotubes [20–22]. Indeed, ss-DNA forms tight helices on carbon nanotubes after sonication of the hybrids, although the role of base dependance and nanotube chirality is still debated [21–23], and raises issues about how long-range order is reached. One might speculate about an analogy between such sonication and vibrofluidization in granular systems [30–43]—or magneto-agitation for magnetic materials [40–42], which has been shown to be describable in terms of an effective temperature [41–43]—possibly via an out-of-equilibrium phase transition [44] in a one-dimensional (1D) system with long range interactions [45]. Order could then come from interacting kinks driven to coalesce and annihilate.

Theoretical research has so far concentrated on the chemical physics of the DNA-nanotube interaction [24–26] and structure of the adsorbed polymer [28] as well as on coarse grained modeling of the hybrid [27]. However we know of no physics-based analysis rooted in the topology of the problem. Yet one sees how topological properties, as well as—or more so than—local considerations, might be quite relevant in such problems of winding helices.

We begin here to explore some topological implications on the unwinding and rewinding of strings in cylindrical geometries, which—we suspect—might be useful in a more general fashion. We describe the low-energy physics of these systems in terms of the Newtonian dynamics of their kinks; analysis of an overdamped, driven regime will be reported elsewhere [47]. Within a minimal, mesoscale, continuum model (M1), we attempt to conceptualize the statics and low-energy nonlinear dynamics of a charged polymer physio-adsorbed on a nanotube. Conclusions are corroborated by numerical analysis of a ball-and-spring model (M2).

II. FRAMEWORK

A. Model 1: Analytical

We start with M1. Consider a 2D field $\boldsymbol{\psi}(s,t)$ which describes a string (polymer) constrained to the surface of a cylinder or radius r: in cylindrical coordinates z,r,θ we have $\psi_1 = z, \psi_2 = r\theta$ (see Fig. 1). Since s is the intrinsic coordinate of the string, as such, $\boldsymbol{T} = \boldsymbol{\psi}'$ is its tangent vector in the space $r\theta,z$.

*cristiano.nisoli@gmail.com, cristiano@lanl.gov

 ©2015 American Physical Society

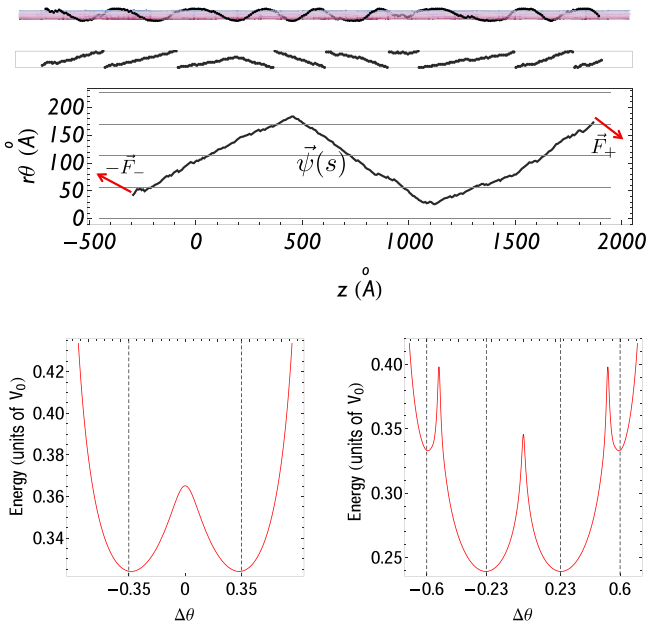

FIG. 1. (Color online) Helical solitons separating helices of different winding angle. The string is shown in three dimensions (top), in cylindrical coordinates (second panel), and in repeated cylindrical coordinates (third panel) which illustrates the curve $\boldsymbol{\psi}(s)$. At the bottom the energy of a helical structure as a function of its gain angle $\Delta\theta$ (radians) between consecutive monomers, for two different choices of σ, with (right) and without (left) metastable states.

We write for $\boldsymbol{\psi}(s,t)$ the following Lagrangian density:

$$\mathcal{L} = \tfrac{1}{2}\lambda\dot{\boldsymbol{\psi}}^2 - \tfrac{1}{2}k(\partial_s \boldsymbol{T})^2 - V(\boldsymbol{T}) \qquad (1)$$

(we denote time derivatives with a dot), where λ is the linear density of mass, k the *effective* bending rigidity, and V an energy that depends only on the tangent vector; we thus assume that the long wavelength dynamics of polymers provides an effective smoothed potential, which affords us an analytical analysis. In a more realistic setup, a site dependent potential will be used in a ball-and-spring model (M2) of which M1 is the continuum generalization. The rigidity k in the bending term is indeed effective. As we will see, when M1 is used to describe M2, the bending term comes from self-interaction of the polymer (screened by the tube) on top of a possible intrinsic bending rigidity of the polymer itself.

Naturally, V contains the possible symmetry breaking of the chiral structure. Its specific form is not relevant to our considerations, as long as it has more than one minimum. It can have the form of a double dip, thus providing for two stable helices, oppositely winding and degenerate (Fig. 1, bottom left). More generally, e.g., because of a corrugation potential of the tube, V can have nondegenerate *local* minima corresponding to different (meta)stable helices (Fig. 1, bottom right).

B. Model 2: Numerical

Before proceeding we motivate M1 by introducing M2, a more faithful ball-and-spring model of nonlocally interacting monomers of cylindrical coordinates θ_i, z_i, which we use in dynamical simulations.

Monomers i and $i+1$ interact harmonically via $K(d_{i,i+1} - a)^2/2$ (d_{ij} is their distance) so that the chain is floppy, as for ssDNA. They also interact repulsively via a screened coulomb potential $U_{ij} = \sigma_{ij} V_o \exp(-d_{ij}/d_o)/d_{ij}$. The modulation factor $\sigma_{ij} = \sigma(\theta_{ij})$ reflects the cylindrical nature of the screening from the tube as well as possible effects of adhesive optimization well known in the case of ssDNA-nanotube hybrids [27]. (Clearly, a is in general slightly smaller than the actual equilibrium length of a straight polymer, because of the electrostatic repulsion.)

We choose a sufficiently smooth function of period π, $\sigma_1(\theta) = [1 + \cos(\theta/2)^2]/2$. In general one can imagine that a corrugation potential can introduce an extra angle beside the one induced by self-interaction and screening. Thus, to conceptualize a metastable state we also consider $\sigma_2 = [1 + \cos(6\theta)^2]/2$. More parametrized choices might be needed to faithfully address specific situations, yet they do not qualitatively change our results.

In simulations we choose $r = 9, a = 7, d_o = 100, V_o = 10$, and $K = 1$, which corresponds, if lengths are measured in Å, to charged ssDNA on a nanotube of diameter of 1.8 nm, with a Debye screening length of 10 nm. We choose $V_o/K = 10$ to ensure an electrostatic stretch of less than 10% of a. The actual value of V_o simply defines the timescale (in the ratio V_o/m with the mass m of the monomer).

Figure 1, bottom left, shows the double-dip shape of the total energy of M2 *when restricted to a helical configuration*, as a function of the wrapping angle, when we choose $\sigma = \sigma_1$ as screening function. Physically, the two opposite stable angles (which depend on r/a) come from a competition: winding the helix increases the screening, but also the repulsion between monomers whose distance is shortened. Figure 1, bottom right shows the helical energy in the case of σ_2, demonstrating the existence of metastable configurations.

Now we can justify the locality in M1 as an approximation of M2, which is obviously nonlocal. Because we study low energy dynamics on helical manifolds separated by kinks, we approximate the total energy with the last two terms in Eq. (1): one, $V(\boldsymbol{T})$, is the energy of the helix (Fig. 1), which depends on its pitch defined by $\boldsymbol{T}$; then the self-repulsion in M2 provides to M1 a term of extra effective bending rigidity. In practice the total energy of M1 is a functional of $\boldsymbol{T}(s)$ and the last two terms in Eq. (1) represent the first two terms of a functional expansion in the derivatives of $T(s)$. The agreement between analytical solutions of M1 and numerics on M2 (see the analysis below) confirms the choice.

III. ANALYTICAL SOLUTIONS, NUMERICAL CORROBORATIONS

(Quasi)degeneracy implies kinks between (meta)stable structures. Before investigating numerically their Newtonian dynamics, we gain theoretical insight by solving M1.

A. Equations of motion

The equations of motion for a string of length $2l$ derived from M1 are obtained by minimizing the constrained

Lagrangian

$$L = \int_{-l}^{l} \left[\mathcal{L} - \frac{1}{2}\mu(\boldsymbol{T}^2 - 1) \right] ds + \boldsymbol{F}_+ \cdot \boldsymbol{\psi}(l) - \boldsymbol{F}_- \cdot \boldsymbol{\psi}(-l), \tag{2}$$

where $\mu(s)$ is a functional Lagrange multiplier ensuring $\boldsymbol{T}(s)^2 = 1\ \forall s$, $\boldsymbol{F}_+$ is the force exerted at one boundary $\boldsymbol{\psi}(+l)$ and $-\boldsymbol{F}_-$ at the other boundary $\boldsymbol{\psi}(-l)$. This returns the equation of motion

$$\lambda \ddot{\boldsymbol{\psi}} = -\partial_s \boldsymbol{j}, \quad \boldsymbol{j}|_{\pm l} = -\boldsymbol{F}_\pm, \tag{3}$$

which is in fact a conservation equation for the density of momentum $\lambda\dot{\boldsymbol{\psi}}$, of flux

$$\boldsymbol{j} = -\partial_{\boldsymbol{T}} V + k\partial_s^2 \boldsymbol{T} - \mu \boldsymbol{T}. \tag{4}$$

If V has local minimum in $\bar{\boldsymbol{T}}$, then the stable helix $\boldsymbol{\psi}(s) = \bar{\boldsymbol{T}}s$ is a static solution. Such a solution exists when the forces applied at the extremities are purely tensile and balanced, $\boldsymbol{F}_\pm = \bar{\boldsymbol{T}}F$. Since $\boldsymbol{j}$ is the stress vector of our 1D system, Eq. (4) shows that the functional Lagrange multiplier $\mu(s)$ is in fact the scalar tensile stress. For a stable helix it is, from Eq. (4), the only stress $\mu(s) = \text{const} = F$. Clearly $\boldsymbol{\psi}(s) = \bar{\boldsymbol{T}}s + \boldsymbol{w}t$ would also be a solution, corresponding to a translating or rotating helix.

Immediately Eqs. (3) show that a helical structure can change its pitch via uniform compression or expansion. Indeed $\boldsymbol{T}(t) = \bar{\boldsymbol{T}}e^{i\omega t}$ (a uniform rotation of the tangent vector in the complex plane representation of 2D vectors) is a solution which corresponds to $\boldsymbol{\psi}(s,t) = \boldsymbol{T}(t)s + \boldsymbol{w}t$. Then, if we substitute it into Eqs. (3) we obtain the tension $\mu(s) = \mu_0 - s^2\omega^2/2\lambda$, where μ_0 is a constant which depends on the forces applied at the boundaries: from Eqs. (3) we have for the tangentially applied forces at the boundaries $\boldsymbol{T}_\pm \cdot \boldsymbol{F}_\pm = \mu_0 - l^2\omega^2/\lambda$, whereas the normally applied forces account for the needed torque: $\boldsymbol{N}_\pm \cdot \boldsymbol{F}_\pm = \partial_{\boldsymbol{T}} V$ (where $\boldsymbol{N} = \boldsymbol{T}'$). This solution is clearly problematic as stresses diverge with size and so does speed ($\dot{\boldsymbol{\psi}}_\pm = \pm l\omega \boldsymbol{N} + \boldsymbol{w}$); it is thus only viable for a finite structure, with properly applied loads.

B. Topological solitons

However, a helical structure can also change its pitch by propagating a soliton. A traveling solution of Eqs. (3) and (4) has the form $\boldsymbol{\psi} = \boldsymbol{\phi}(s - vt) + \boldsymbol{w}t$, which implies $\boldsymbol{T} = \boldsymbol{\phi}'$.

Then Eqs. (3) become $\lambda v^2 \boldsymbol{T}' = -\boldsymbol{j}'$ which can be integrated to obtain

$$k\boldsymbol{T}'' = -\partial_{\boldsymbol{T}} W(\boldsymbol{T}) + \mu \boldsymbol{T}. \tag{5}$$

Equation (5) is simply a Newton equation for a "particle" described by $\boldsymbol{T}(s)$ (where now s is "time" in the equivalent Newton picture) constrained to a circumference (because $\boldsymbol{T}^2 = 1$) and subject to the potential

$$W(\boldsymbol{T}) = -V(\boldsymbol{T}) + \tfrac{1}{2}\lambda v^2 (\boldsymbol{T} - \boldsymbol{\tau})^2. \tag{6}$$

Here $\boldsymbol{\tau}$ is defined by

$$\boldsymbol{F}_- = \lambda v^2 (\boldsymbol{T}_- - \boldsymbol{\tau}) \tag{7}$$

where $\boldsymbol{T}_\pm = \boldsymbol{T}(\pm l)$.

Equation (5) becomes more manageable if projected on its Frennet-Serret reference frame [48]. We define α via $\boldsymbol{T} = e^{i\alpha}$, and similarly $\boldsymbol{\tau} = \tau e^{i\alpha_\tau}$. Then projection on the normal vector $\boldsymbol{N} = \boldsymbol{T}'$ yields finally

$$k\alpha'' = -\partial_\alpha W(\alpha). \tag{8}$$

The above is a simple 1D Newton equation for a particle moving in a potential,

$$W(\alpha) = -V(\alpha) + \lambda\tau v^2[1 - \cos(\alpha - \alpha_\tau)], \tag{9}$$

but is now an unconstrained one. Its solution returns α and thus $\boldsymbol{T}$ and from that $\boldsymbol{\phi} = \int \boldsymbol{T}\, ds$.

Instead, projection on the tangent $\boldsymbol{T}$ returns the tensile stress

$$\mu = \lambda v^2 (1 - \boldsymbol{\tau} \cdot \boldsymbol{T}) - k\alpha'^2. \tag{10}$$

From Eqs (8) and (10), via linearization, the phonon dispersion in a stable helix $\bar{\alpha}$ is readily found to be

$$\omega^2 = c_F^2 q^2 + (k/\lambda) q^4, \tag{11}$$

where $c_F^2 = c^2 + F/\lambda$ is the tension-dependent speed of sound, and c is the speed of sound in absence of tension, given by $c^2 = \partial_{\bar{\alpha}}^2 V|_{\bar{\alpha}}/\lambda$. Without the direction-dependent potential $V(\boldsymbol{T})$ the helical angle would be defined by the direction of the opposite tensile forces at the boundaries, and we would also have $c_F^2 = F/\lambda$, the well known speed of sound for a string under tension. Note also that the helical structure is stable to applied pressure ($F < 0$) when it does not exceed the critical value $-F > \lambda c^2$.

Moving to solitons, we are now in familiar territory. If we consider $l \to \infty$ then a topological soliton connecting two different stable or metastable helical structures corresponds to a trajectory between two *degenerate* maxima of W [3,5], as shown in Fig. 2. These helices are associated with (possibly local) minima of V.

Indeed, when $v = 0$, and the kink is static, from Eq. (6) $W = -V$ and maxima of W are minima of V and correspond to stable helices; static kinks are thus only possible between *degenerate* structures of the same energy (unless of course proper forces are applied at the end, thus changing the energetics). However, dynamical solitons between nondegenerate structures are also possible, as we shall see in the next subsection.

C. Locked speed

So far we have reduced the problem of a traveling solution to an equivalent Newton equation. In this context, the soliton is a special trajectory between two degenerate maxima of a properly defined potential energy. That is of course typical in problems of topological solitons (consider the sine-Gordon case) or tunneling [3,49,50].

However Eq. (6) has an interesting feature missing in most such problems. There is an extra term in W, proportional to the square of the speed (see also Fig. 2, top panel), which implies that even if two helices do not have the same energy, a kink can still exist between them *but it must travel, and with a locked speed*. Indeed only $v \neq 0$ in the second term of Eq. (6) can make the effective potential W degenerate when V is not. This is much different from the case of a sine-Gordon soliton, and other similar cases, where the potential W does not depend on

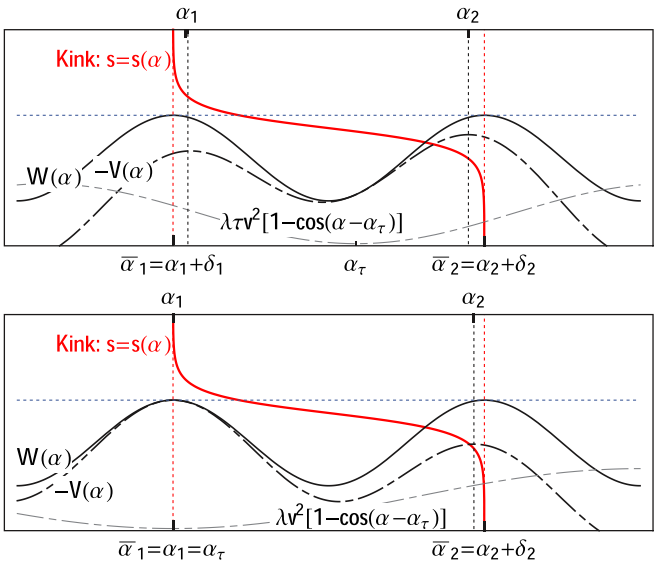

FIG. 2. (Color online) Schematics of a solution of Eq. (8). Top: in general a soliton correspond to a trajectory connecting two maxima of W (solid black line). From Eq. (6), maxima of W do not correspond to minima of V (dashed black line), due to the extra term $\lambda\tau v^2[1-\cos(\alpha-\alpha_\tau)]$ (dashed grey line). It follows that solitons between degenerate structures are possible but they must have a specific speed. Bottom: the solution for a soliton between helices of different energy V, the same as that obtained by simulations shown in Fig. 3 (see Supplemental Material S1 [46]).

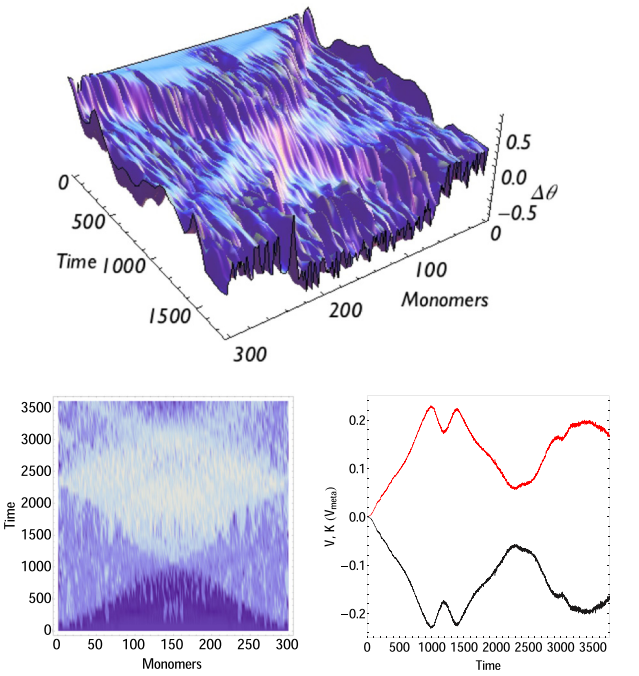

FIG. 3. (Color online) Helical solitons separating helices of different winding angle, propagating into a region of higher potential energy (numerical integration of the Newtonian dynamics of M2, animation in Supplemental Material S1 [46]). The system starts in a metastable helical configuration (Fig. 1, bottom right panel). Stable helical configurations form at the boundaries and propagate inside. Top: 3D plot for the angular deviation $\Delta\theta_i = \theta_{i+1} - \theta_i$ vs space and time. Bottom left: density plot for the angular deviation $\Delta\theta_i = \theta_{i+1} - \theta_i$ (also plotted in 3D at the bottom) as a function of time and monomers, demonstrating propagation at fixed speed, collision, and reflection on the boundaries. Bottom right: the time evolution of kinetic (red) and potential (black) energy (V_m is the energy of the initial metastable configuration) demonstrates the expected initial linear growth of kinetic energy until collision; after collision a stable helix of opposite orientation forms with solitons now propagating outward until reflection.

the speed of the soliton, and as a consequence only solitons between degenerate structures exist, and at any speed below the speed of sound [5].

The physical reason for this mechanism is rather intuitive. The propagation of a soliton corresponds to a homotopy between continuum states of different topological invariant (winding angle) per unit length. This constrains a rotation of one domain with respect to the other.

For a heuristic understanding, consider a soliton propagating inside a static region (2) of higher energy, leaving a helix of lower energy (1) in its wake. Because of continuity, helix B must rotate with respect to A, with speed $\dot{\boldsymbol{\psi}}_1 = v(\boldsymbol{T}_2 - \boldsymbol{T}_1)$. As the soliton propagates at constant speed v, the total kinetic energy increases linearly in time with rate $\lambda v^3(\boldsymbol{T}_2 - \boldsymbol{T}_1)^2/2$ while the potential energy decreases linearly in time with rate $(V_2 - V_1)v$. Then energy conservation locks the speed of the soliton at

$$v^2 = 2\frac{V_1 - V_2}{\lambda(\boldsymbol{T}_1 - \boldsymbol{T}_2)^2}. \tag{12}$$

Thus, the kinetic energy necessary for the rotation of one helix with respect to the other is provided by the energy difference between the two domains, and the soliton effectively turns potential energy into kinetic energy as it propagates at constant speed. If, however, the two domains are degenerate, the soliton must be static.

Remarkably, this heuristic formula precisely returns the correct speed v that makes W of Eq. (6) degenerate (having chosen $\boldsymbol{\tau} = \boldsymbol{T}_1$, or $\boldsymbol{F}_- = 0$). This can be seen clearly in Fig. 2, bottom panel, which predicts the existence of a soliton of speed v given by (12) between nondegenerate (meta)stable helices.

Speed locking clarifies that in these system energy and momentum are not localized inside the soliton (as in a sine-Gordon case), but rather flow through the soliton as it propagates. This can also be understood from Eqs. (3) from which we have $\boldsymbol{j} = \lambda v^2(\boldsymbol{T}_1 - \boldsymbol{T})$; the flux of momentum is uniform in the helical structures but changes through the soliton.

We use M2 to corroborate this result. Figure 3 shows results of a velocity-Verlet numerical integration of M2. A helix is prepared in a metastable state corresponding to $\Delta\theta \simeq 0.6$ rad (Fig. 1, bottom right panel), with open boundaries. Lower energy helices ($\Delta\theta \simeq 0.23$ rad) form at the boundaries and propagate inside with constant speed, as the potential energy decreases linearly, and the kinetic energy correspondingly increases. We see from the simulation that upon collision a new metastable helix ($\Delta\theta \simeq -0.6$ rad) forms and the potential energy starts increasing again, until reflection with the boundaries. As the simulation proceeds more energy from the solitonic dynamics is dissipated into phonons, as expected in a discrete system (see Supplemental Material S1 [46]).

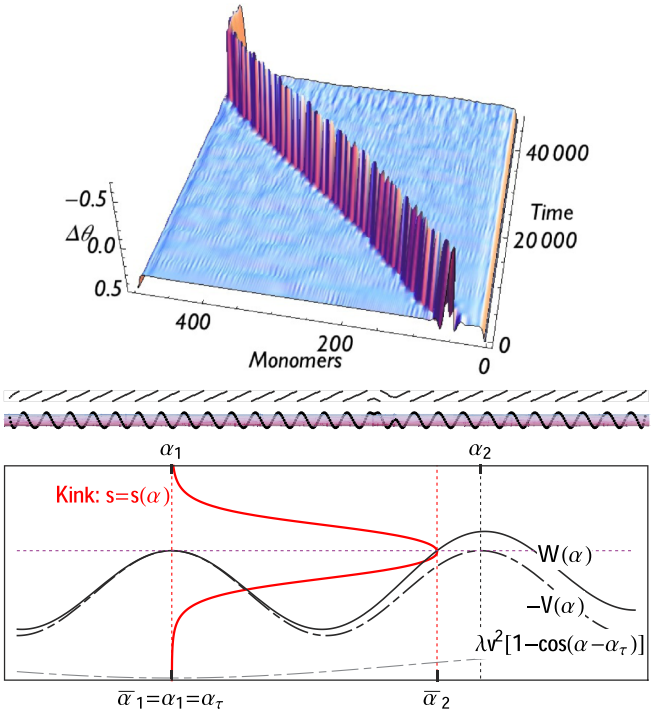

FIG. 4. (Color online) Pulse soliton propagating at uniform speed, obtained by velocity-Verlet integration of M2. Top: plot of the angular deviation $\Delta\theta_i = \theta_{i+1} - \theta_i$ between consecutive monomers as function of time. Below we show a snapshot of the pulse in cylindrical coordinates and in 3D. A pulse soliton is predicted by our analytical framework M1 (bottom panel) as the speed v raises the maximum in $V(\alpha_2)$, allowing for a trajectory that bounces back from α_2 and returns to α_1. As $v \to 0$ the size of the pulse increases, ultimately tending to two static kinks places infinitely far away.

D. Pulses

While this topological soliton can only propagate at locked speed, the union of a kink-antikink separates two identical domains with no relative rotation of the two and can thus—at least in principle—propagate at any speed.

Indeed such pulses are admitted by our analytical framework M1. Consider for instance two degenerate minima of V, α_1 and α_2, as in Fig. 4. We choose $\boldsymbol{F}_- = 0$ and thus $\boldsymbol{\tau} = \boldsymbol{T}_- = \boldsymbol{T}_1$. Now W has still a maximum in α_1, but a higher maximum in $\alpha_2 + \delta$ slightly shifted from α_2. A trajectory can now start in α_1, reach the proximity of the new structure, and then come back to α_1, thus describing a kink-antikink pair (Fig. 4, bottom panel).

Clearly an upper limit for v must exist. Much like in the sine-Gordon cases, it is given by the speed of sound of the helical structure, although the underlying reason is in fact different. Indeed in our case, when $v^2 > c^2 = \partial_\alpha^2 V$, α_1 is not a maximum of W anymore but rather a minimum, and thus and no solitonic solution is possible. Instead, in sine-Gordon-like solitons the presence of an upper limit for the speed of any soliton, and not just pulses, comes from the pseudo-relativistic invariance of the Lagrangian. In Fig. 4 we show results of simulations on M2 demonstrating stability and motion of such pulses (see Supplemental Material S2 for a movie [46]).

Note that as v goes to zero, and $W(\alpha_2)$ becomes degenerate with $W(\alpha_1)$, the trajectory in Fig. 4 (bottom) describes two opposite kinks progressively far away from each other. It is not difficult (details will be shown elsewhere [47]) to compute the total energy for a traveling pulse of speed v and to obtain that, in the limit of low speed, the energy decreases. When $v \to 0$ it tends to the energy of two static kinks, placed infinitely far away and thus noninteracting.

Since in a discrete system soliton propagation is associated with phonon radiation, one would predict that a pulse will always decay into two distant static kinks. However, we can see how topology, again, protects from this dynamics: an increase in the size of the pulse must force a relative rotation on the identical helices separated by the pulse. As those are assumed to be infinitely long, the kinetic energy cost would be infinite.

For finite systems, however, the decay is possible; indeed simulations of exactly the same situation depicted in Fig. 4, but on 300 rather than 500 monomers, show such decay (Supplemental Material S3 [46]), as the energy needed to set the external domain into rotation is inferior to the energy stored in the bound kink-antikink.

Finally, note that in Fig. 4, and therefore in the discussion above, $V(\alpha_2) = V(\alpha_1)$. However when $V(\alpha_2) > V(\alpha_1)$ there is a minimum speed for the pulse, given by Eq. (12), corresponding to the speed that makes W degenerate, with $W(\bar{\alpha}_2) = W(\bar{\alpha}_1)$. Everything said above for the case $v \to 0$ generalizes to this case when v tends to its minimum value.

IV. CONCLUSIONS

We have shown that topological solitons in strings of different helical structures afford a description as particle-like excitations. Indeed, while the collective rotation of domains might make it seem impossible to describe the low-energy physics in terms of excitation dynamics (kinks), still such a picture can be regained by folding the domain dynamics into a velocity dependent effective potential for the kinks, which thus places constraints on their speed.

These solitons are stable but different from, e.g., sine-Gordon-like solitons: unlike the latter, they can separate nondegenerate structures. Their velocities are controlled by a competition between the kinetic energy of helical rotation and steady changes in potential energy due to helical wrapping or unwrapping, and are proportional to the square root of the energy difference of the two domains, and inversely proportional to the scalar difference of the tangent vectors that define the helicity of each domain. Bound couples of kinks and antikinks form pulses that can travel at any speed between a minimum and a maximum (the speed of sound of the structure).

A wealth of work covers the subject of solitons in double or multiple well potentials, and it is related to the quantum problem of tunneling, topological defects and in general transitions between solutions that are homotopically distinct from the vacuum [3,5,49,50]. In general, in sine-Gordon-like problems in one dimension, it is shown that a solitonic solution corresponds to a pseudo-trajectory for a classical Newtonian particle, traveling between two degenerate maxima of $-V$ where V is a nonlinear, multiple well potential for the degree of freedom of the problem. As we know the sine-Gordon or

double-well-Gordon equations are invariant under a boost of the Poincaré group, which allows solitonic solutions at any speed below the speed that defines the group: there the speed of the soliton gauges the mass of the Newtonian particle. Here, however, the potential energy does not depend on the degree of freedom but rather on its derivative, which defines a preference for wrapping and a preferred wrapping angle. Mathematically this translates in the same pseudo-Newton picture for the soliton as a classical trajectory, but now the speed of the soliton does not contribute to the mass of the pseudo-trajectory, rather it adds to the energy of the structure an extra term that depends on the speed of the soliton itself. Thus it is not $-V$ that need to be degenerate but W of Eq. (6), allowing solitons between nondegenerate structures, and at the same time locking the speed. This simple picture reflects the physical fact that energy (and momentum) is not contained *in* the soliton, but rather flow through the soliton, and is contained in the domains which the soliton separates, where it is transformed from potential to kinetic energy as the soliton passes by. This nonlocality of energy can nonetheless be subsumed into the usual picture of a Newtonian pseudo-trajectory.

ACKNOWLEDGMENTS

We are grateful to S. Kilina and D. Yarotski for useful discussions. The work was supported by U.S. DOE BES E304, KAW and ERC DM 321031, under the auspices of the National Nuclear Security Administration of the U.S. DOE at Los Alamos National Laboratory under Contract No. DEAC52-06NA25396.

[1] A. Shapere, and F. Wilczek, *Geometric Phases in Physics*, Vol. 14 (World Scientific, Singapore, 1989).
[2] D. R. Nelson, *Defects and Geometry in Condensed Matter Physics* (Cambridge University Press, Cambridge, 2002).
[3] P. M. Chaikin and T. C. Lubensky, *Principles of Condensed Matter Physics* (Cambridge University Press, Cambridge, 1995).
[4] L. D. Landau *et al.*, *Course of Theoretical Physics: Theory of Elasticity* (Pergamon Press, Oxford, 1959).
[5] T. Dauxois and M. Peyrard, *Physics of Solitons* (Cambridge University Press, Cambridge, 2010).
[6] M. J. Ablowitz and H. Segur, *Solitons and the Inverse Scattering Transform* (SIAM, Philadelphia, 1981).
[7] G. P. Alexander *et al.*, Rev. Mod. Phys. **84**, 497 (2012).
[8] M. Freedman, Bull Am. Math. Soc **40**, 31 (2003).
[9] F. Wilczek, Nat. Phys. **5**, 614 (2009).
[10] J. M. Kosterlitz and D. J. Thouless, J. Phys. C: Solid State Phys. **6**, 1181 (1973).
[11] C. Nisoli and A. R. Bishop, Phys. Rev. Lett. **112**, 070401 (2014).
[12] C. Nisoli, N. M. Gabor, P. E. Lammert, J. D. Maynard, and Vincent H. Crespi, Phys. Rev. Lett. **102**, 186103 (2009).
[13] C. Nisoli, N. M. Gabor, P. E. Lammert, J. D. Maynard, and Vincent H. Crespi, Phys. Rev. E **81**, 046107 (2010).
[14] C. Nisoli, Phys. Rev. E **80**, 026110 (2009).
[15] I. Adler *et al.*, Ann. Bot. **80**, 231 (1997); R. V. Jean, *Phyllotaxis: A Systemic Study in Plant Morphogenesis* (Cambridge University Press, Cambridge, England, 1994).
[16] L. S. Levitov, Phys. Rev. Lett. **66**, 224 (1991).
[17] A. Amir, J. Paulose, and D. R. Nelson, Phys. Rev. E **87**, 042314 (2013).
[18] K. A. Williams *et al.*, Nature (London) **420**, 761 (2002).
[19] J. Couet *et al.*, Angew. Chem. Int. Ed. **44**, 3297 (2005).
[20] M. Zheng *et al.*, Nat. Mater. **2**, 338 (2003).
[21] M. Zheng *et al.*, Science **302**, 1545 (2003).
[22] B. Gigliotti *et al.*, Nano Lett. **6**, 159 (2006).
[23] D. A. Yarotski *et al.*, Nano Lett. **9**, 12 (2009).
[24] R. R. Johnson *et al.*, Nano Lett. **8**, 69 (2008).
[25] R. R. Johnson *et al.*, Nano Lett. **9**, 537 (2009).
[26] R. R. Johnson *et al.*, Small **6**, 31 (2010).
[27] S. Manohar, T. Tang, and A. Jagota, J. Phys. Chem. C **111**, 17835 (2007).
[28] S. Kilina *et al.*, J. Drug Delivery **2011**, 415621 (2011).
[29] C. J. Gannon *et al.*, Cancer **110**, 2654 (2007).
[30] H. M. Jaeger, S. R. Nagel, and R. P. Behringer, Rev. Mod. Phys. **68**, 1259 (1996).
[31] B. Behringer, Nature (London) **415**, 594 (2002).
[32] A. R. Abate and D. J. Durian, Phys. Rev. Lett. **101**, 245701 (2008).
[33] P. Sollich, F. Lequeux, P. Hebraud, and M. E. Cates, Phys. Rev. Lett. **78**, 2020 (1997).
[34] V. Colizza, A. Barrat, and V. Loreto, Phys. Rev. E **65**, 050301 (2002).
[35] C. M. Song, P. Wang, and H. A. Makse, Proc. Natl. Acad. Sci. **102**, 2299 (2005).
[36] L. F. Cugliandolo, J. Kurchan, and L. Peliti, Phys. Rev. E **55**, 3898 (1997).
[37] A. Mehta and S. F. Edwards, Physica A **157**, 1091 (1989).
[38] H. A. Makse and J. Kurchan, Nature (London) **415**, 614 (2002).
[39] G. D'Anna *et al.*, Nature (London) **424**, 909 (2003).
[40] R. F. Wang *et al.*, Nature (London) **439**, 303 (2006).
[41] C. Nisoli, R. Wang, J. Li, W. F. McConville, P. E. Lammert, P. Schiffer, and V. H. Crespi, Phys. Rev. Lett. **98**, 217203 (2007).
[42] C. Nisoli, J. Li, X. Ke, D. Garand, P. Schiffer, and V. H. Crespi, Phys. Rev. Lett. **105**, 047205 (2010).
[43] L. F. Cugliandolo, J. Phys. A: Math. Theor. **44**, 483001 (2011).
[44] M. R. Evans, Brazil. J. Phys. **30**, 1 (2000).
[45] M. E. Fisher, S.-k. Ma, and B. G. Nickel, Phys. Rev. Lett. **29**, 917 (1972).
[46] See Supplemental Material at http://link.aps.org/supplemental/10.1103/PhysRevE.91.062601 for animations.
[47] C. Nisoli A. V. Balatsky (unpublished).
[48] J.-A. Serret, J. de Math. **16**, 193 (1851).
[49] A. Barone *et al.*, Nuovo Cimento **1**, 227 (1971).
[50] H. Kleinert, *Path Integrals in Quantum Mechanics, Statistics, Polymer Physics, and Financial Markets* (World Scientific, Singapore, 2009).